

# Photofragment-excitation spectrum of NO<sub>2</sub> observed through O(<sup>3</sup>P<sub>*J*</sub>) detection

Jun Miyawaki, Kaoru Yamanouchi and Soji Tsuchiya

*Department of Pure and Applied Sciences, College of Arts and Sciences, The University of Tokyo, Komaba, Meguro-ku, Tokyo 153, Japan*

Received 25 January 1991; in final form 11 March 1991

Photodissociation dynamics of NO<sub>2</sub> was investigated by observation of the photofragment-excitation (PHOFEX) spectrum of NO<sub>2</sub> obtained by detecting O(<sup>3</sup>P<sub>*J*</sub>; *J*=2, 1, and 0). Near the photodissociation threshold, the average branching ratios of three spin-orbit sublevels were consistent with those predicted by a restricted statistical distribution model, in which the predissociation rate to produce O atoms in each spin-orbit state is proportional to the limited number of energetically allowed states of the NO fragment.

## 1. Introduction

In our previous report [1], the spin-orbit state distribution of O(<sup>3</sup>P<sub>*J*</sub>) (*J*=2, 1, and 0) formed by photolysis of NO<sub>2</sub> was investigated at fixed photolysis wavelengths at 355, 337, 266, and 212 nm and a large deviation from the statistical distribution of <sup>3</sup>P<sub>2</sub>:<sup>3</sup>P<sub>1</sub>:<sup>3</sup>P<sub>0</sub>=1:0.6:0.2 was observed. The photolyses at 355, 337, and 266 nm yielded a similar distribution, i.e. <sup>3</sup>P<sub>2</sub>:<sup>3</sup>P<sub>1</sub>:<sup>3</sup>P<sub>0</sub> ≈ 1:0.19:0.03, while that at 212 nm yielded 1:0.35:0.08. The difference in the distributions was ascribed to the existence of the dissociation channel, NO+O(<sup>1</sup>D), which is open only for the 212 nm photolysis. On the other hand, in the recent investigation by Robra, Zacharias and Welge [2], photofragment-excitation (PHOFEX) spectra for a counterpart fragment of NO(<sup>2</sup>Π<sub>1/2</sub>, *v*=0, *j*) exhibited characteristic structures near the threshold region of the respective channels with a different rotational quantum number *j*. This threshold structure observed for the NO fragment must also be reflected in the formation of the O(<sup>3</sup>P<sub>*J*</sub>) fragment in respective *J* states.

In the present study, in order to obtain further insight into the predissociation mechanism, PHOFEX spectra are observed through detection of O(<sup>3</sup>P<sub>*J*</sub>) in respective *J* states. Based on the excess-energy dependence of the branching ratios to three spin-orbit

states and of the width of the peaks, the predissociation of NO<sub>2</sub> is investigated especially in the near-threshold region.

## 2. Experimental

In the measurement of the laser-induced-fluorescence (LIF) and PHOFEX spectra near the threshold region, rotationally cold NO<sub>2</sub> was produced in a supersonic jet formed by expansion of an NO<sub>2</sub>(0.2%)/He mixture with a stagnation pressure of 5 atm into a vacuum chamber through a pulsed nozzle (General Valve 9-279-900) with orifice diameter of 0.8 mm.

Three dye lasers were simultaneously excited by an XeCl excimer laser (Lambda Physik EMG101MSC) and two (Lambda Physik FL3002E) of them were used to generate a tunable VUV laser for detection of O(<sup>3</sup>P<sub>*J*</sub>) and the other one (Moletron DL16) was used as a photolysis laser with tunable wavelength. For generation of the VUV laser at around the 130 nm region, a scheme of two-photon resonance difference frequency mixing was adopted with a non-linear medium of Kr [1,3]. The generated VUV laser beam was introduced into a vacuum chamber through a LiF prism. The resolution of the VUV laser was 0.5 cm<sup>-1</sup> [1,3], which was suffi-

ciently high to monitor separately the  $^3S_1-^3P_J$  ( $J=2, 1, \text{ and } 0$ ) transitions, respectively, at 130.2, 130.5 and 130.6 nm. The wavelength dependence of the VUV laser intensity was calibrated in advance with respect to the intensity of one of the dye-laser beams whose wavelength was varied. During the experiment, the intensities of the laser beams mixed in Kr were monitored to calibrate the VUV laser intensity.

The photolysis laser beam and the VUV laser beam were collinearly counter-propagated with each other and crossed the jet perpendicularly. The VUV laser beam was optically delayed by 10 ns from the photolysis laser. The photofragment of O( $^3P_J$ ) from NO<sub>2</sub> was detected by a LIF signal of the  $^3S_1-^3P_J$  transitions. The fluorescence was collected by a solar-blind photomultiplier (Hamamatsu R1259) placed in the direction perpendicular to both of the laser beam and jet axes. The signal was amplified by a preamplifier (NF BX-31) and averaged by a boxcar integrator (Stanford SR250). In order to record a PHOFEX spectrum for O( $^3P_J$ ), the wavelength of the photolysis laser was scanned by fixing the VUV laser wavelength at each of the  $^3S_1-^3P_J$  transitions.

Distances between the nozzle orifice and the laser beam were 32 and 10 mm for the LIF and PHOFEX measurements, respectively. In the LIF measurement, the rotational temperature of NO<sub>2</sub> was 0.9 K, and then, almost all NO<sub>2</sub> (98%) molecules were populated at the 0<sub>00</sub> rotational level and the concentration of the rotationally hot NO<sub>2</sub> at the 2<sub>02</sub> level was only 2%. In the experimental condition for the PHOFEX spectrum, the rotational temperature achieved was 3 K, and 75% and 25% of NO<sub>2</sub> were populated at the 0<sub>00</sub> and 2<sub>02</sub> levels, respectively. The above rotational temperatures were derived from the rotational structure of a LIF spectrum of NO<sub>2</sub> observed at 593 nm under the same experimental conditions. Concentration of N<sub>2</sub>O<sub>4</sub> in the NO<sub>2</sub>/He mixture, estimated from the equilibrium constant of the dimerization process, was 6%. However, its contribution in the spectra can be neglected because an absorption cross section of N<sub>2</sub>O<sub>4</sub> is more than 10 times smaller than that of NO<sub>2</sub> in this energy region [4]. Furthermore, the photon energy of the UV light employed in this experiment is insufficient for photodissociation of N<sub>2</sub>O<sub>4</sub> to produce O( $^3P$ ).

### 3. Results and discussion

#### 3.1. LIF and PHOFEX spectra near the threshold

In fig. 1, the PHOFEX and the LIF spectra are compared in the photodissociation threshold region between 25105 and 25155 cm<sup>-1</sup>. A sudden decrease of the fluorescence intensity of NO<sub>2</sub> at 25130.6 cm<sup>-1</sup>, which was determined from the PHOFEX spectrum of NO<sub>2</sub> observed by detecting NO in the lowest level ( $^2\Pi_{1/2}, v=0, j=0.5$ ) [2], indicates that the fluorescence quantum yield drops to zero due to opening of the lowest dissociation channel. Below the threshold, two peaks are recognized in the PHOFEX spectrum. These two peaks can be ascribed to photodissociation of rotationally hot NO<sub>2</sub> populated at the 2<sub>02</sub> level.

It is known that the  $^2B_2$  state of NO<sub>2</sub> interacts strongly with the electronic ground  $^2A_1$  state [5]. A zeroth-order vibronic level of the  $^2B_2$  state splits into a number of levels by coupling with high vibrational levels of the  $^2A_1$  state. Thus, the observed peaks in the LIF spectra represent the vibronic levels of NO<sub>2</sub> formed by mixing of the  $^2B_2$  and  $^2A_1$  states. Since the PHOFEX spectrum has a spectral structure similar to that observed in the LIF spectrum below the dissociation threshold, it is obvious that the photodissociation process of NO<sub>2</sub> in the observed energy region is a predissociation through a certain quasi-bound state of the vibronically excited levels.

In the energy region shown in fig. 1, peaks in the PHOFEX spectrum are considerably broader than those in the LIF spectrum just below the dissociation threshold. The broadening of the peaks in the PHOFEX spectrum simply reflects the homogeneous line broadening due to a dissociation reaction. As described later, the width of the peaks in the PHOFEX spectrum tends to be broader as energy increases.

#### 3.2. Branching ratios to three spin-orbit states of O( $^3P_J$ )

The PHOFEX spectra of NO<sub>2</sub>, observed by detecting O( $^3P_2$ ), O( $^3P_1$ ), and O( $^3P_0$ ) in the energy region between 25100 and 25650 cm<sup>-1</sup>, are shown in fig. 2a. The threshold energies for O( $^3P_1$ ) and O( $^3P_0$ ) are higher by 158 and 226 cm<sup>-1</sup> [6], respectively, than that for O( $^3P_2$ ). The intensity dis-

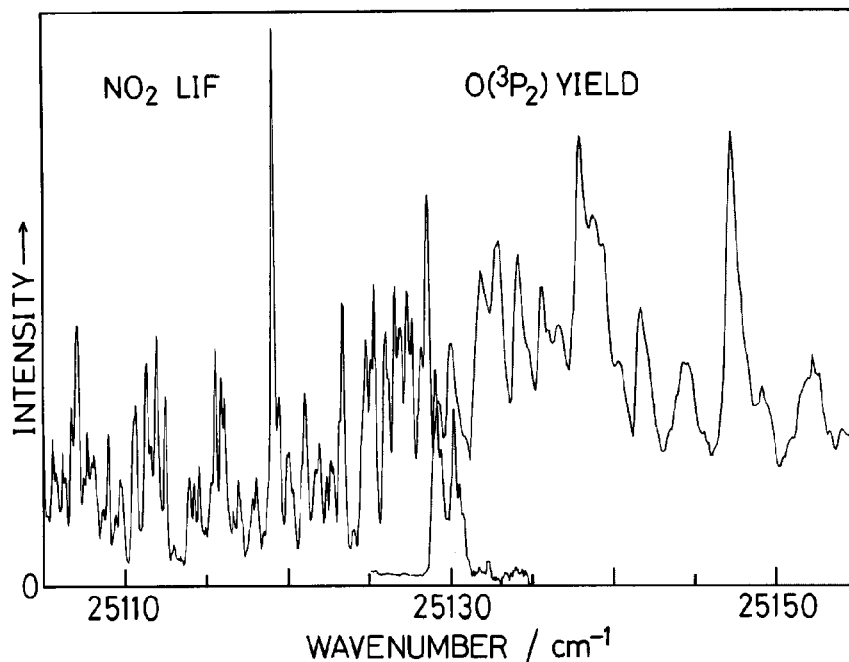


Fig. 1. LIF and  $O(^3P_2)$ -monitored PHOFEX spectra of  $NO_2$  in the photodissociation threshold region between 25105 and 25155  $cm^{-1}$ . The rotational temperature of  $NO_2$  in the LIF spectrum is about 0.9 K and the population of rotational levels other than the lowest rotational level  $O_{00}$  is negligibly small (2%). The rotational temperature of  $NO_2$  in the PHOFEX spectrum is 3 K and the  $O_{00}$  and  $2_{02}$  levels have populations of 75% and 25%, respectively. Thus, the wavelength, where the sudden drop of the LIF intensity is observed, corresponds to the dissociation threshold.

tributions for these three spectra indicate some common features, i.e. there are relatively intense peaks at the same excitation energies. For example, peaks are commonly observed in the three spectra at 25460, 25525, 25535, 25580, and 25608  $cm^{-1}$ . These peaks indicate that quasi-bound vibronic levels of  $NO_2$  exist and transition probabilities to these levels are relatively large. However, relative intensities of these peaks are different in the three spectra, and furthermore, some peaks recognized in one spectrum do not appear in another spectrum. In order to examine a variation of the branching ratios to the three channels as a function of the excitation energy, the ratio of  $f_J = I(^3P_J)/I(^3P_2)$  ( $J=1$  or  $0$ ) is derived as shown in fig. 2b, where  $I(^3P_J)$  represents a relative population of  $O(^3P_J)$ , which is calculated using the observed intensity of the PHOFEX spectrum in fig. 2a and the oscillator strengths of  $O(^3S_1-^3P_J)$  transitions ( $f=0.031, 0.032, \text{ and } 0.031$  for  $J=2, 1, \text{ and } 0$ , respectively) [6]. Though both of  $f_1$  and  $f_0$  fluctuate

significantly, the ratios increase gradually towards a higher energy region, while their slopes tend to decrease as energy increases.

If the branching ratio is proportional to the number of energetically allowed channels,  $n_J$ , for  $O(^3P_J)$ ,  $f_J$  can be calculated by  $n_J/n_2$  ( $J=1$  or  $0$ ) as shown in fig. 2b. Here,  $n_J$  is derived by counting energetically allowed ro-vibronic levels of  $NO$ , taking account of the statistical weights of  $O(^3P_J)$  and  $NO$ . The calculated ratios,  $n_1/n_2$  and  $n_0/n_2$ , are larger by approximate factors of 3 and 7, respectively, than the observed  $f_1$  and  $f_0$ , and their slopes decrease gradually and converge to their statistical limits of 0.6 and 0.2, respectively.

In our previous study [1],  $f_1=0.19$  and  $f_0=0.03$  were derived as averages for the photolyses at 355, 337 and 266 nm, whose excess energies measured from the dissociation threshold are around 3060, 4540, and 12460  $cm^{-1}$ , respectively. This result implies that effective channel numbers for production

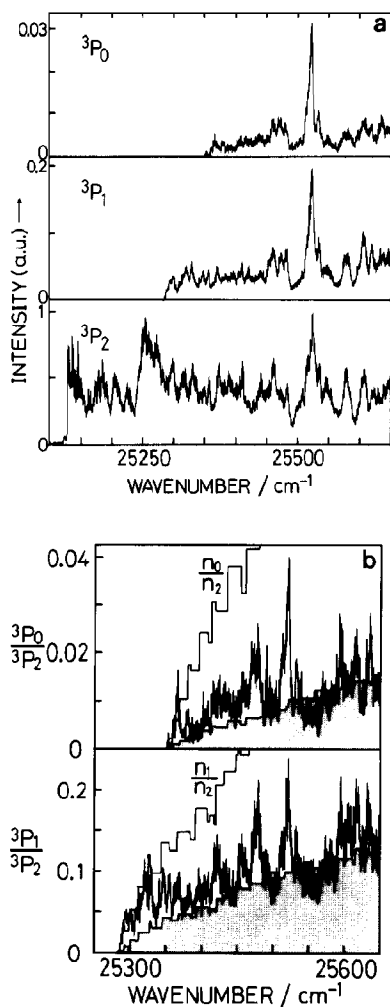


Fig. 2. (a) The PHOFEX spectra for  $O(^3P_J, J=2, 1, \text{ and } 0)$  produced from  $\text{NO}_2$  for the photolysis energy region of  $25100\text{--}25650\text{ cm}^{-1}$ ; (b) the observed branching ratios of  $f_1 = I(^3P_1)/I(^3P_2)$  (a lower trace) and  $f_0 = I(^3P_0)/I(^3P_2)$  (an upper trace) as a function of the photolysis laser wavelength. The calculated ratios for numbers of energetically open channels,  $n_1/n_2$  (a lower trace) and  $n_0/n_2$  (an upper trace) are also plotted by staircase lines. In each trace, a staircase line with a hatched region indicates a restricted statistical ratio, i.e.  $0.32(n_1/n_2)$  for a lower trace and  $0.15(n_0/n_2)$  for an upper trace.

of O atoms in the  $^3P_1$  and  $^3P_0$  states relative to that for the  $^3P_2$  are proportional to the relative number of the energetically open channels multiplied by limitation factors, 0.32 and 0.15 for  $J=1$  and  $J=0$ , respectively. It is found that the limited branching ra-

tios,  $0.32(n_1/n_2)$  and  $0.15(n_0/n_2)$ , plotted in fig. 2b, represent well the overall features of  $f_1$  and  $f_0$ .

The fact that the observed branching ratios are approximately proportional to the number of the repulsive dissociation channels suggests that the predissociation rate constant,  $k(\delta E)$ , could be described by a statistical theory similar to the RRKM theory, i.e.

$$k(\delta E) = W(\delta E)/hN(E), \quad (1)$$

where  $\delta E$  is the excess energy above the dissociation threshold,  $N(E)$  is the level density of excited  $\text{NO}_2$ , and  $W(\delta E)$  is the number of the rotation-vibration states of excited  $\text{NO}_2$  in the transition state. In this narrow energy region, the variation of the density of states of  $\text{NO}_2$  as a function of energy can be disregarded. Then, the predissociation rate should increase monotonically with the excitation energy in proportion to the number of rovibrational levels of the transition state. Since the predissociation occurs just after the excitation energy exceeds the dissociation threshold, the transition state of  $\text{NO}_2$  may be connected to the open channels for the dissociation without a barrier, and therefore,  $W(\delta E)$  in eq. (1) can be approximated by the number of open channels giving NO and  $O(^3P_J)$  at the excess energy of  $\delta E$ .

The limitation factors estimated above suggest that only a limited number of channels among the energetically allowed ones can take part in the predissociation process. In view of the overall feature, the branching ratios tend to converge to the restricted statistical values. Then, it can be concluded that the limitation factors introduced in the analysis represent the restrictions caused by conservation of the electronic angular momentum.

The branching ratio in the energy region where strong peaks are found in fig. 2a is larger in general than the restricted statistical values. One example is an intense peak at  $25520\text{ cm}^{-1}$ . The peak may represent a certain quasi-bound rovibronic level which favors the production of O atoms with a  $J$  distribution closer to the statistical one. Two mechanisms are possible to explain this finding. One is that nuclear motions, such as an overall rotation and an internal rotation in the course of the predissociation from this level, induce couplings with the electronic motion to affect the partitioning of the nuclear and

electronic angular momenta. The other is that the dissociation lifetime of the excited  $\text{NO}_2$  in this level is long enough for interactions among all allowed channels to yield a  $J$  distribution closer to the statistical one.

### 3.3. Predissociation rate

The PHOFEX spectrum of  $\text{NO}_2$  obtained by detecting  $\text{O}(^3\text{P}_2)$  is shown in fig. 3 in the photolysis energy region of  $25100\text{--}27300\text{ cm}^{-1}$ . It is noticed that the peak width tends to be broader as the photolysis energy increases, indicating a large dissociation rate for larger excess energy. In order to discuss the broadening effect quantitatively, a peak is adopted for measurement of its width only when two adjacent minima have intensities less than 60% of the peak intensity. The width is defined as an fwhm of the Lorentzian function which fits the peak shape above the adjacent two minima, where a base line of the Lorentzian function is located at zero-intensity level of the spectra. In fig. 4, the peak widths are

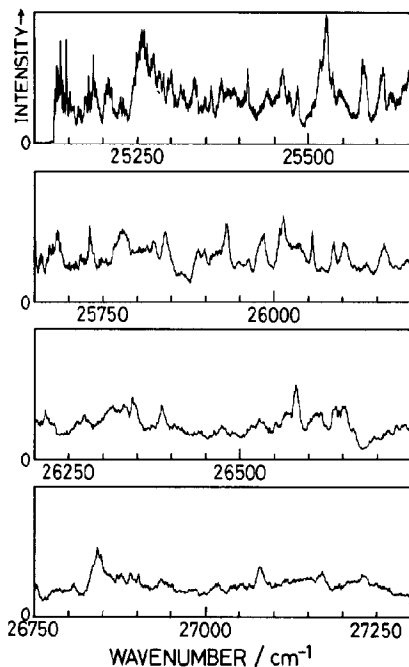


Fig. 3. The PHOFEX spectrum for  $\text{O}(^3\text{P}_2)$  from  $\text{NO}_2$  for the photolysis energy region of  $25100\text{--}27300\text{ cm}^{-1}$ .

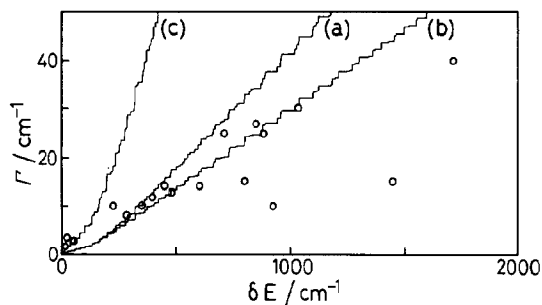


Fig. 4. The linewidth  $\Gamma$  as a function of the excess energy  $\delta E$ . Open circles represent the observed peaks in fig. 3. Curves (a) and (b) respectively show calculated linewidths assuming that the width is proportional to the number of channels,  $n_2 + n_1 + n_0$  and  $n_2 + 0.32n_1 + 0.15n_0$ . A width of  $0.45\text{ cm}^{-1}$  for  $n_2=10$  and  $n_1=n_0=0$  is adopted [7]. Curve (c) represents the linewidth calculated by the RRKM theory.

plotted as a function of the excitation energy.

If it is assumed that the width of the peaks in the PHOFEX spectrum is proportional to the number of energetically open channels,  $n_2 + n_1 + n_0$ , the variation of the peak width as a function of excess energy is calculated as curve (a) in fig. 4. The assumed proportion coefficient of  $0.045\text{ cm}^{-1}$  is the one derived by our recent observation of the PHOFEX spectrum for  $\text{NO}$  fragments in the lowest channels (the degeneracy is 10) of  $\text{NO}(^2\Pi_{1/2}, v=0, j=0.5) + \text{O}(^3\text{P}_2)$  [7], which corresponds to the predissociation rate of  $8.5 \times 10^9\text{ s}^{-1}$ .

Though the observed width should be interpreted as an upper limit due to overlapping of adjacent predissociation levels of  $\text{NO}_2$ , the calculated width is even larger than the observed ones. The restricted statistical model adopted in the analysis of the branching ratio may improve to some extent by reducing the number of available channels. By using the limitation factors of 0.32 and 0.15 for  $\text{O}(^3\text{P}_1)$  and  $\text{O}(^3\text{P}_0)$ , respectively, the effective number of open channels is calculated as  $n_2 + 0.32n_1 + 0.15n_0$  and the calculated width is also plotted in fig. 4 as curve (b). It is possible that all the energetically allowed  $J=2$  channels are not open as is the case estimated for  $J=1$  and  $J=0$  channels; i.e. the limited total channel number may be written as  $R(n_2 + 0.32n_1 + 0.15n_0)$  with  $R < 1$ . Therefore, the observed substantially narrow widths below curve (b) may suggest a restriction of an effective channel

number for formation of  $O(^3P_2)$  from  $NO(^2\Pi_{1/2}, v=0, j)$ .

Assuming the density of states  $N(E)$  of 10 levels/ $\text{cm}^{-1}$ , which is determined from the LIF spectra for the energy region just below the threshold [5], we calculated the width by the RRKM theory using eq. (1); this is also depicted as curve (c) in fig. 4. Overestimation of the width reflects the fact that the LIF spectrum does not sample all the energy levels due to the limited Franck-Condon factors, so that the density of states is underestimated. If the density of state is 35 levels/ $\text{cm}^{-1}$ , the RRKM curve coincides with curve (a) in fig. 4.

#### 4. Conclusion

(1) From the measurement of the PHOFEX spectra of  $NO_2$  by detecting  $O(^3P_J)$ , the branching ratios of three spin-orbit channels,  $^3P_1/^3P_2$  and  $^3P_0/^3P_2$ , are found to be much less than the statistical values, though they fluctuate substantially near the threshold regions for production of the  $J=1$  and  $J=0$  states.

(2) On the other hand, the overall feature of the branching ratios is consistent with that predicted by a restricted statistical distribution model, where the predissociation rate for each spin-orbit channel is proportional to the number of energetically allowed channels of an NO fragment with constant factors of

0.32 and 0.15 for  $^3P_1$  and  $^3P_0$ , respectively.

(3) The broadening of the peaks in the PHOFEX spectrum is hard to deduce quantitatively due to overlapping of neighboring peaks. However, the observed widths as a function of the excess energy are consistent with the restricted statistical model.

#### Acknowledgement

The present work is supported in part by a Grant-in-Aid for Scientific Research on Priority Areas (01606003) and General Scientific Research (02403006).

#### References

- [1] J. Miyawaki, T. Tsuchizawa, K. Yamanouchi and S. Tsuchiya, *Chem. Phys. Letters* 165 (1990) 168.
- [2] H. Zacharias and K.H. Welge, *NATO Ser. B Phys.* 105 (1983) 123; U. Robra, H. Zacharias and K.H. Welge, *Z. Physik D* 16 (1990) 175.
- [3] T. Tsuchizawa, K. Yamanouchi and S. Tsuchiya, *J. Chem. Phys.* 92 (1990) 1560; 93 (1990) 111.
- [4] T.C. Hall Jr. and F.E. Blacet, *J. Chem. Phys.* 20 (1952) 1745.
- [5] H. Nagai, K. Shibuya and K. Obi, *J. Chem. Phys.* 93 (1990) 7656.
- [6] C.E. Moore, *Atomic energy levels*, NSRDS-NBS, Circular No. 35 (US GPO, Washington, 1971).
- [7] J. Miyawaki, K. Yamanouchi and S. Tsuchiya, unpublished results.